Int. J. High Technology Ceramics **4** (1988) 227–241

9

High Temperature Creep Testing of Ceramics

D. F. Carroll* & S. M. Wiederhorn

National Bureau of Standards, Building 223, Gaithersburg, MD 20899, USA

1 INTRODUCTION

To use ceramic materials in structural applications at high temperatures, the design engineer has to be able to predict the creep and creep rupture behaviour of the material under complex load conditions. Creep and creep rupture behaviour of ceramic materials have usually been characterised in flexure because flexural testing is relatively simple and specimen machining costs are low (Cannon *et al.*, 1980; Porter *et al.*, 1981; Grathwohl, 1984). However, there are problems associated with this technique because ceramics tend to creep faster in tension than in compression (Morrell & Ashbee, 1973; Birch *et al.*, 1978; Wiederhorn *et al.*, 1986; Wiederhorn *et al.*, 1988). This asymmetric creep behaviour results in a time-dependent stress and strain distribution in the flexure beam during deformation (Cohrt *et al.*, 1984; Chuang *et al.*, 1987; Chuang & Wiederhorn 1988). The type of complications that arise in a deformed flexure beam can be seen in Fig. 1 which summarises how the creep strain varies throughout a bend beam of siliconised silicon carbide as a function of time. After one hour of deformation under 250 MPa at 1300°C, the creep strain varied linearly throughout the bend beam with approximately the same amount of deformation occurring on both the tensile and compressive sides of the beam. The neutral strain axis after one hour of deformation was found to correspond to the geometric centre of the bend beam (normalised beam position of 0·5). However, after seven hours of deformation, the strain distribution is no longer symmetric about the geometric centre of the bend beam. The deformation on the tensile side of the bend beam is much greater

* Present address: Dow Chemical Company, Central Research Advanced Ceramics Lab., Building 1776, Midland, Michigan, 48674, USA.

Int. J. High Technology Ceramics 0267-3762/88/$03·50

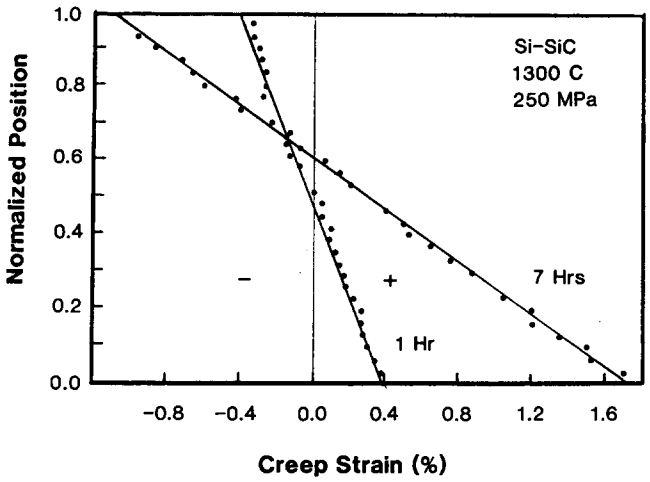

Fig. 1. Creep strain as a function of position in a bend beam. Specimen deformed under 250 MPa at 1300°C for one and seven hours. Normalised beam position of 0·0 and 1·0 corresponds to the tensile and compressive surface of the bend, respectively. Creep strain throughout the bend beam was determined by a technique described by Chen & Chuang (1987).

than on the compressive side. The outer tensile fibre strain was measured to be approximately 1·7% while the outer compressive fibre strain was approximately 0·95%. The neutral strain axis has also shifted from the geometric centre towards the compressive surface of the bend beam to a normalised beam position of 0·6.

Since the neutral strain axis (as well as the neutral stress axis) moves during deformation when a material exhibits asymmetric creep behaviour, flexural creep results cannot be directly used to predict creep behaviour in other stress states unless the movement of neutral axis is taken into consideration. In order to avoid the complications associated with asymmetric creep behaviour, the creep behaviour of a material should be characterised under uniaxial tension and compression. Once characterised, uniaxial creep data can be used to predict creep behaviour in more complex stress states, thereby avoiding the problems associated with predictions from flexural creep results.

The techniques used for tensile and compressive creep testing are not as well-known as the standard flexural creep test. In general, the compressive creep test is relatively simple and has been frequently used to characterise the creep behaviour of ceramic materials (Lange *et al.*, 1980; Cannon & Langdon, 1983; Carter *et al.*, 1984). The tensile creep test, on the other hand, has been used to a more limited extent (Morrell, 1972; Kossowsky *et al.*, 1975; Lange *et al.*, 1979; Govila, 1983; Wakai *et al.*, 1986). In those cases

where tensile creep tests have been conducted, the costs of test fixtures and specimen preparation were one of the limiting factors in these studies. Recently, at the National Bureau of Standards (NBS), inexpensive techniques for measuring the tensile and compressive creep behaviour of materials have been developed. This paper will describe these experimental techniques and briefly summarise some creep results for a two-phase ceramic material.

2 TENSILE CREEP APPARATUS

A schematic representation of the tensile creep apparatus developed at the NBS is shown in Fig. 2. In this apparatus the tensile specimen is attached to two silicon carbide loading rods which extend into the hot zone of the furnace. The specimen is attached to the rods in a pin and clevis arrangement using sintered alpha silicon carbide pins. The SiC loading rods extend out of the furnace and are attached via simple universal joints, to an air piston which applies the load to the specimen (upper rod) and to a load cell which monitors the applied load on the specimen (lower rod).

The grip arrangement used in this apparatus is commonly known as a hot-grip technique because the ends of the silicon carbide loading rods are located inside the furnace and are at test temperature. An advantage of the hot-grip technique is that small tensile specimens are used which minimises

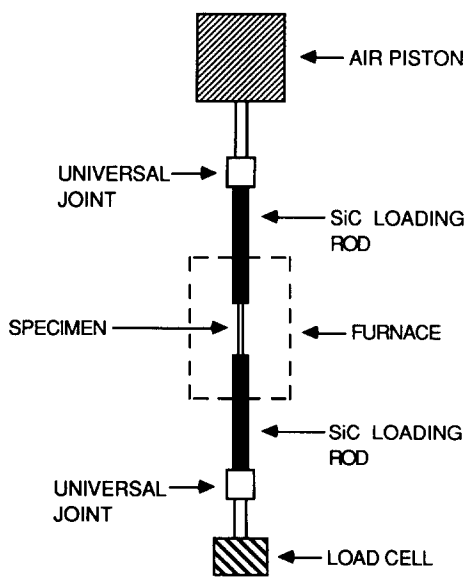

Fig. 2. Schematic representation of the tensile loading apparatus.

specimen costs. In other grip arrangements, specimen costs are greater since long tensile specimens are necessary to extend out of the furnace hot zone to the grips.

2.1 Tensile specimen

The tensile specimen used at NBS (Fig. 3(A)) is a flat dogbone shaped specimen with a hole at each end. The holes are used to pin the specimen to the silicon carbide loading rods. The tensile specimens have a gauge length of approximately 20 mm with a cross-sectional area of 2·5 by 2·5 mm. As shown in Fig. 4, the specimens are made by a simple grinding technique, in which a block of material with the same dimensions as the length and width of the desired tensile specimens is reduced in cross-section with a shaped grinding wheel. The shaped grinding wheel leaves the cross-section of the block identical to the cross-section of tensile specimen. A thin wafering saw is then used to cut tensile specimens from the block to the desired thickness.

The next step is to machine the holes into the specimens. This is a crucial step because the degree of alignment in the tensile specimen is dependent upon the ability to machine the holes accurately and uniformly on the centreline of the specimen. If the material has a high enough conductivity, as

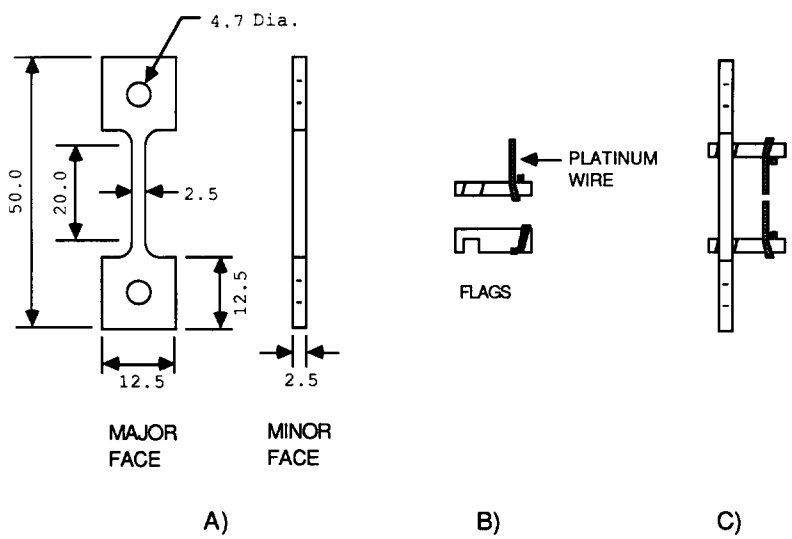

Fig. 3. (A) schematic representation of the major and minor faces of the flat dogbone-shaped tensile specimen. Tensile specimen is attached to loading rods using a pin and clevis arrangement. (B) schematic representation of the flags used in creep measurement technique. (C) flags attached to the gauge section of specimen. The flags contacts the specimen along two lines forming a well defined gauge length. Idea of flags originated by Chuck (1986).

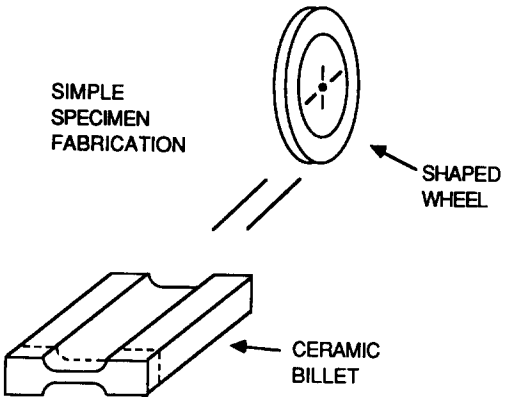

Fig. 4. Schematic of method used to produce test specimens by simple grinding and cutting technique. A shaped grinding wheel is used to cut the cross-section of the test specimen, after which specimens are cut by slicing perpendicular to the cross-section of the blank.

in the case of siliconised or reaction-bonded silicon carbides, electro-discharge machine (EDM) techniques may be used. If the holes are machined using an EDM technique, total specimen costs are approximately three times the cost of a conventional bend beam. However, when EDM cannot be used (silicon nitrides, aluminas, etc.), specimen costs are higher since more conventional methods must be used to machine the holes into the specimens.

2.2 Creep strain measurement

Creep deformation is measured directly on the gauge section of the test specimen. A high resolution telescope with a working distance of approximately 150 mm was used to view the gauge section of the specimen through an opening of the furnace. The gauge length of the specimen was marked with a set of alpha silicon carbide flags attached to the gauge section. Figure 3(b) is a schematic representation of the flags. The flags were made by cutting an angled slot about the size of the specimen cross-section into a rectangular piece of alpha silicon carbide. At the other end of the flag a piece of platinum wire was attached. The slotted end of the flag was then placed around the gauge section of the specimen. If everything was machined properly the flags were held into place by frictional forces. The flags contact the specimen along two lines (Fig. 3(c)) forming a well-defined gauge length. A room temperature cement was used to secure the flags to the gauge section, so the specimen could be placed into the furnace without disturbing the position of the flags. During furnace heat-up, the cement was burned off leaving the flags held in place by frictional forces. At elevated temperatures, oxidation and sintering secured the flags to the gauge section. Figure 5 shows

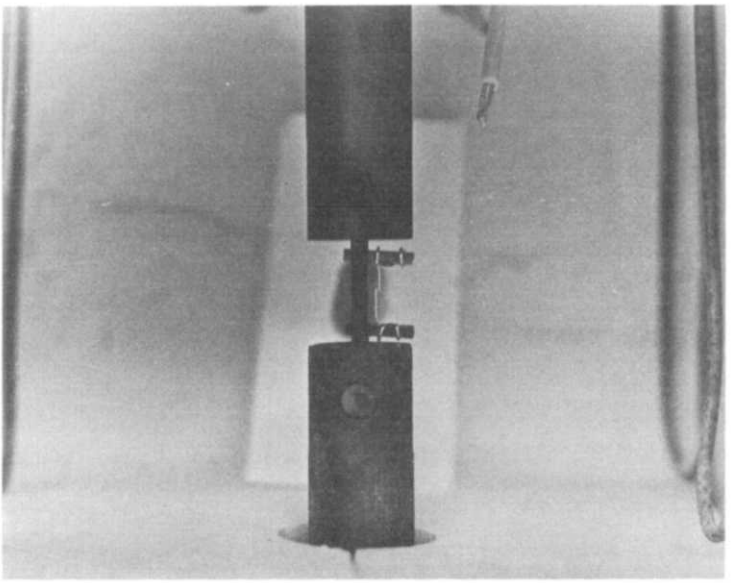

Fig. 5. Tensile specimen is pinned to the SiC loading rods that penetrate the furnace. Flags with platinum wires can be seen attached to the specimen's gauge section.

a tensile specimen in the furnace with the flags attached to the gauge section. Creep strain was measured by focusing the telescope on the ends of the platinum wires, which were made visible at elevated temperatures by removing some of the insulation from the furnace wall directly behind the specimen. This procedure created a cool background, thus enabling the platinum wires to be distinguished from the interior of the furnace. Using this technique, creep displacements could be measured to an accuracy of ± 2 microns at 1300°C.

In the future, an automated system for measuring creep strain will be incorporated into this tensile creep apparatus. A laser extensometer will be used to measure the displacement continuously with time. Again, the alpha silicon carbide flags will be used to mark the gauge section of the specimen; however, in this case, the platinum wires will not be used. The laser extensometer will scan in a vertical line through a window in the furnace. The laser beam will be interrupted by the two alpha silicon carbide flags as it passes through another window in the furnace to a detector. The detector can sense the interruption of the laser by the flags and so measure the specimen's gauge length. The laser extensometer will record the movement of gauge length as a function of time within an accuracy of ± 2 microns.

2.3 Alignment

One of the major concerns in the development of a tensile creep apparatus is specimen alignment. An excellent review paper by Christ & Swanson (1978)

has identified many of the sources responsible for misalignment and gives examples of how to minimise bending moments that are introducted by the tensile load train. A common source for misalignment in the pin and clevis design of the NBS apparatus is shown in Fig. 6(A). The pin used to attach the specimen to the silicon carbide loading rod does not sit properly in the hole but rests on the edge of the tensile specimen. This type of misalignment introduces a bending moment into the major face of the tensile specimen. In order to minimise this possibility the holes of the specimens are tapered (Fig. 6(B)) by using a simple grinding technique that involves 30 micron diamond paste, oil and a cone-shaped, copper rod attached to a slow speed drill press. It is important that the holes are tapered the same amount from each side so that the load will be applied to the centre of the specimen.

If the pins sit properly in the holes, alignment about the minor face of the specimen is limited by how close the holes are machined to the centreline of the specimen (Fig. 6(C)). An analysis by Christ & Swanson (1978) can be used to estimate how much bending will be introduced in the specimen if the holes are offset from the centreline. Using their analysis, the amount of bending due to either eccentric or cantilever loading can be kept to less than 5% if the holes are machined to $\pm 0{\cdot}025$ mm and $\pm 0{\cdot}050$ mm of the centreline,

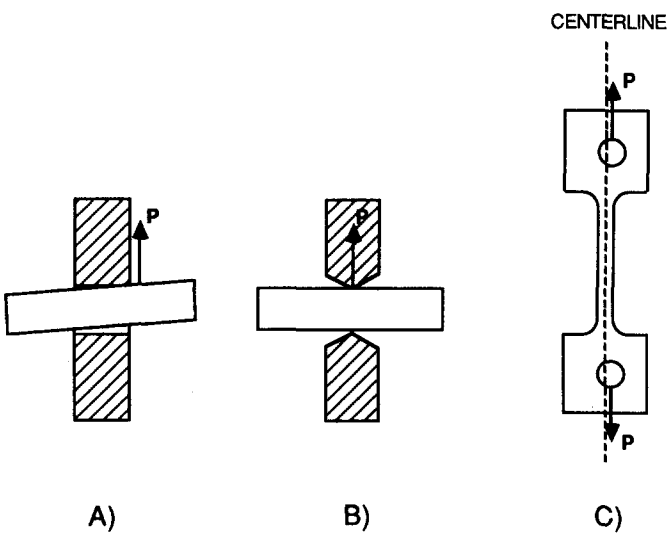

Fig. 6. Schematic representation showing common sources of and solutions for misalignment in the pin and clevis gripping technique. (A) misalignment caused by the pin resting on edge of tensile specimen. A bending moment is produced in the major face of the specimen. (B) A solution for the type of bending shown in (A). The holes in the tensile specimen are tapered so that the load is applied to the centre of the specimen. (C) misalignment caused by the holes being machined off the centreline of the tensile specimen. This type of misalignment produces a bending moment about the minor face of the specimen.

respectively. For careful machining practices, electro-discharge methods (EDM) can routinely machine the holes to within $\pm 0{\cdot}025$ mm of the centreline.

The degree of misalignment in the tensile specimens was determined by measuring the elastic strain of the gauge section as a function of applied stress at room temperature. In order to characterise the amount of bending that accompanies a tensile load, the elastic strains on all four sides of the gauge length need to be measured simultaneously about the same perimeter of the gauge section (Christ & Swanson, 1978). However, due to the small cross-section of the gauge length, it was extremely difficult to attach four strain gauges to the same perimeter of the gauge section. Therefore, the degree of misalignment was determined by measuring the strain variation between opposite sides of the specimen. By using this technique, the amount of bending about either the major or minor face of the specimen could be determined. In this analysis, a total of four different specimens were examined. The results shown in Fig. 7 are for a specimen which exhibited the most bending.

Figure 7 summarises the percent bending about the major and minor faces of a specimen as a function of applied stress. The percent bending between two opposite faces was calculated using:

$$\% \text{ Bending} = \left| \frac{\varepsilon_1 - \varepsilon_0}{\varepsilon_0} \right| \times 100\% \tag{1}$$

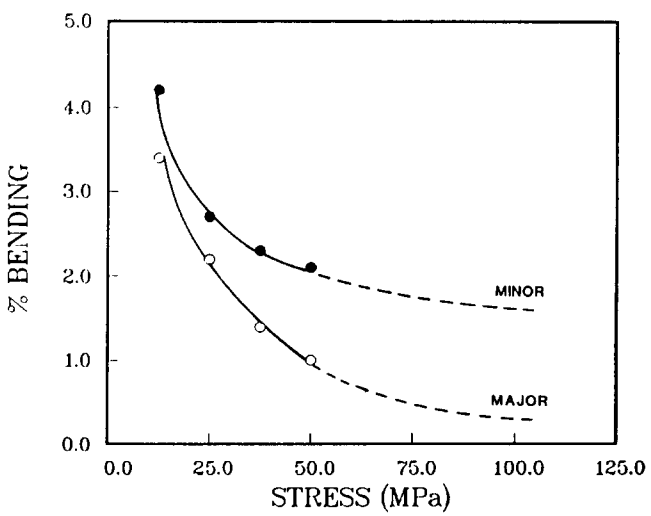

Fig. 7. The percent bending about the major (○) and minor (●) faces of a tensile specimen with tapered holes, as a function of applied stress.

where ε_1 was the elastic strain from one side of the specimen, ε_2 the elastic strain from the opposite side of the specimen and ε_0 the average strain determined by $(\varepsilon_1 + \varepsilon_2)/2$.

The percent bending about the major face of the specimen was found to decrease from a high of approximately 3·3% at 12·5 MPa to approximately 1% at 50 MPa. Higher stresses were not applied to the specimen for fear of brittle fracture at room temperature. The applied stresses used in the tensile creep tests at elevated temperatures generally exceeded 75 MPa. An extrapolation of the elastic strain data to these stress levels showed that the percent bending about the major face of the specimen should be less than 1%. This result indicates that very good alignment is obtained about the major face of the specimen, using the tapered holes shown in Fig. 6(B).

For the case of the minor face, the percent bending was shown to decrease from approximately 4·2% at 12·5 MPa to 2·1% at 50 MPa. At the stress levels used in the creep tests, the percentage bending about the minor face of the specimen should be less than 2%. Using the analysis by Christ & Swanson (1978), this amount of bending corresponds to holes which were machined to within 0·025 mm of the centreline.

Another check for good alignment is to measure the curvature of the specimen after deformation. Ideally, any small elastic stress variations due to misalignment should even out as the material undergoes deformation. However, bending in the specimen may still occur if there is an off-axis translation of the upper grip as the specimen deforms. Even though displacements of the upper grip are quite small ($<0{\cdot}175$ mm), it is still necessary to check the curvature of the specimen to ensure alignment is maintained during deformation. The amount of bending after deformation was measured using a device developed by Jakus & Wiederhorn (1988). The device consisted of a stylus attached to a linear variable differential transducer (LVDT). As the specimen is translated under the stylus, the displacement of the surface from a plane is determined by the LVDT. Surface curvature as a function of distance along the gauge section is then calculated directly from the displacement data. The equipment is capable of measuring surface displacements over distances of 50 mm to an accuracy of 1 micron. The equipment is controlled by a computer so that the curvature can be calculated automatically from the data.

The curvature along the major face of a tensile specimen before and after deformation is shown in Fig. 8(A) and (B), respectively. In Fig. 8(A), the curvature of the as-machined specimen is essentially zero with only a slight variation with position on the specimen. The slight variation in curvature along the gauge section is a consequence of surface roughness from the machining process. After deformation to a creep strain of approximately 0·25%, there is little change in the overall curvature of the gauge section

(Fig. 8(B)). The maximum radius of curvature along the gauge section is measured to be approximately 17 m. If the specimen exhibited a uniform radius of curvature of 17 m, the amount of strain in the specimen due to bending would be approximately 2% of the total measured creep strain. These results confirm that there is little bending introduced into the tensile specimen and that alignment is maintained during deformation. Similar curvature results were obtained for the minor face of the tensile specimen.

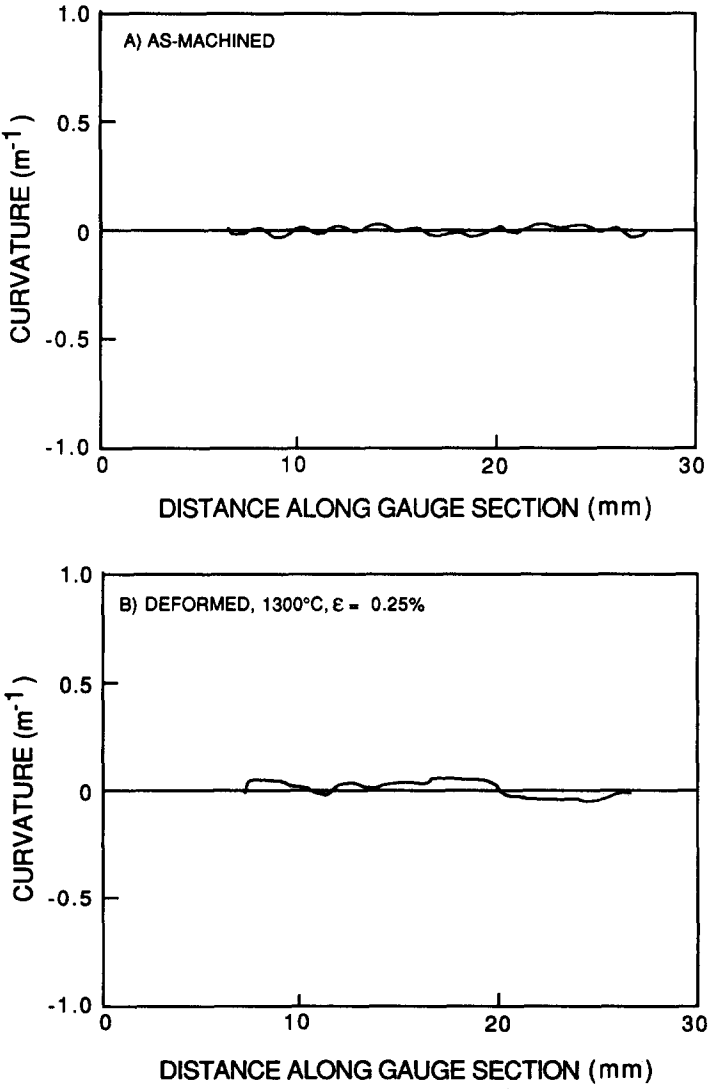

Fig. 8. Curvature of a tensile specimen with tapered holes as a function of distance along the gauge section. (A) as-machined specimen. (B) deformed at 1300°C to a creep strain of approximately 0·25%. Curvature is expressed as $1/R$, where R is the radius of curvature.

3 COMPRESSIVE CREEP APPARATUS

The experimental configuration for compressive creep testing is shown in Fig. 9. Rectangular specimens approximately 8 × 3 × 3 mm were mounted between two pedestals made out of alpha silicon carbide. The upper pedestal was rounded so that a point contact would direct the load through the centre of the specimen. The upper pedestal was rounded by gently hand polishing with 15 micron diamond paste on a soft lap. Hand holding the pedestal during polishing assured that the centre of the pedestal became raised relative to the edges. Two large blocks of alpha silicon carbide were then placed between the pedestals and the loading rods in order to prevent damage to the latter. Finally, to prevent sticking of the alpha silicon carbide blocks to the silicon carbide loading rods, thin discs of aluminium oxide were used as spacers. The load was applied and maintained by means of a screw-driven testing machine.

Creep measurements in compression were made with the same high powered telescope used in the tensile creep tests. However, in this case, the telescope was focused on either the edges of the pedestals or on the edges of alpha silicon carbide fibres that were attached to the pedestals. Again, a cool spot was formed on the rear wall of the furnace by removing some of the furnace insulation. This procedure created a dark background which enabled the edges of the pedestals or fibres to be seen.

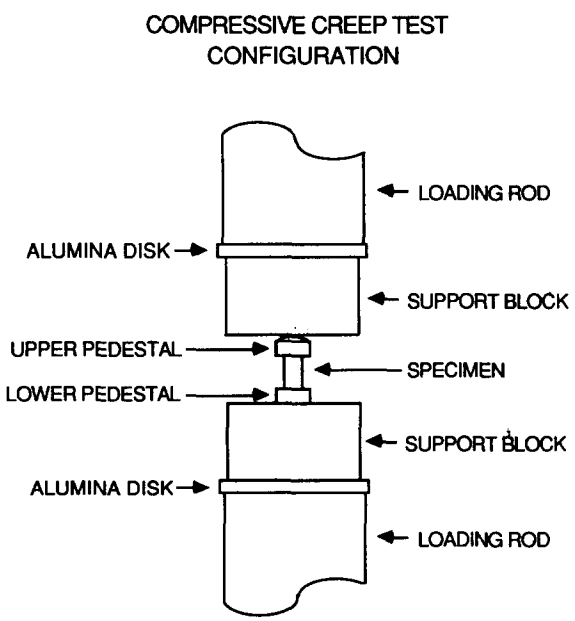

Fig. 9. Experimental configuration for compressive creep apparatus.

4 CREEP RESULTS FOR A REACTION BONDED SILICONISED SILICON CARBIDE

A comparison of the steady-state creep rate in tension and compression of a reaction bonded siliconised silicon carbide at 1300°C is given in Fig. 10. The material used in this study contained approximately 33 volume percent silicon and 67 volume percent silicon carbide in the form of 2 to 5 micron SiC grains distributed randomly throughout the silicon matrix. A distinct increase in slope of a logarithmic plot of steady-state creep rate versus applied stress is observed for both the tension and compressive creep results, indicating a greater sensitivity to creep at high stresses than at low stresses (Wiederhorn *et al.*, 1988). For creep in tension, the data can be represented by two straight lines. Above 100 MPa the stress exponent is approximately 12, whereas below 100 MPa the stress exponent is approximately 4. These data are similar to the results obtained by Carroll & Tressler (1988) at 1100°C. In tension, the increase in slope has been attributed to creep cavities which nucleate rapidly enough above 100 MPa to contribute significantly to the creep rate. For creep in compression, the data can also be divided into a low stress regime having a stress exponent of four and a high stress regime having a stress exponent of 13. In compression, the increase in the slope of the creep curve cannot be attributed to cavitation, since no cavities were observed in this material under compression (Wiederhorn *et al.*, 1988).

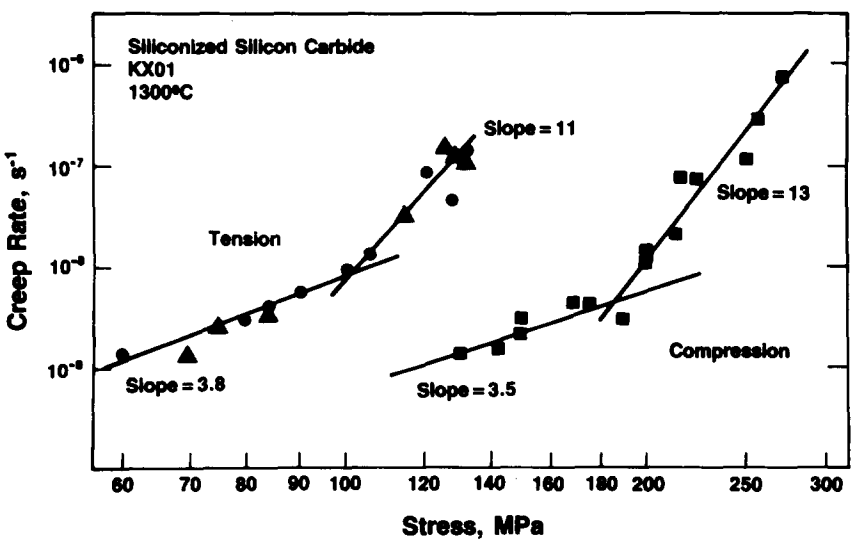

Fig. 10. Stress dependence of the creep rate for a reaction bonded silicon carbide tested under tension and compression at 1300°C. Both the tensile and compressive creep data follow bimodal curves. Material is much more creep resistant in compression than in tension.

Results of transmission electron microscopy indicate an enhancement of dislocation activity in the silicon carbide grains at these high compressive stresses, suggesting a role of plastic deformation in the creep process (Hockey & Wiederhorn, 1988).

Although the shape of the creep curves obtained in tension and compression are similar, the results demonstrate a greater creep resistance under compressive loading. A comparison between the low stress segments of each curve indicates that for a given applied stress, the creep rate in tension is at least twenty times greater than the creep rate in compression. This difference is even greater if the creep rate in the high stress segment of the tension curve is compared to the low stress segment of the compressive curve. At 150 MPa, the creep rate in tension is approximately 400 times that in compression. The reasons for the difference in creep under tension and compression have been discussed elsewhere (Wiederhorn *et al.*, 1988; Hockey & Wiederhorn, 1988).

5 SUMMARY

In this paper, techniques used at the National Bureau of Standards for measuring the tensile and compressive creep behaviour of structural ceramics were described. The tensile creep apparatus was based upon a hot-grip technique which employed a pin and clevis arrangement to attach the specimen to the loading train. Good alignment was obtained in the load train through careful machining and tapering of the specimen holes. The percentage of elastic bending in the tensile specimen was measured to be less than 1% and 2% about the major and minor faces of the specimen, respectively. The creep deformation was measured using a high-powered telescope to follow the movement of flags attached to the specimen's gauge section. The compressive creep apparatus consisted of a screw-driven testing machine which applied the load to a specimen through a series of rounded pedestals and loading blocks. Compressive creep deformation was measured using a technique similar to that in tension. Tensile and compressive creep measurements were then described for a reaction bonded silicon carbide at 1300°C.

ACKNOWLEDGEMENT

This work was supported by the US Department of Energy. Ceramic Technology for Advanced Heat Engines Program under Interagency Agreement DE-AI05-850R21569.

REFERENCES

Birch, J. M., Wilshire, B. & Godfey, D. J. (1978). Deformation and fracture processes during creep of reaction bonded and hot pressed silicon nitride. *Proc. Brit. Ceram. Soc.*, **25**, 141–54.

Cannon, W. R. & Langdon, T. G. (1983). Review: creep of ceramics, Part 1, mechanical characteristics. *J. Mat. Sci.*, **18**, 1–50.

Cannon, R. M., Rhodes, W. H. & Heuer, A. H. (1980). Plastic deformation of fine grained alumina (Al_2O_3): I, interface-controlled diffusional creep. *J. Am. Ceram. Soc.* **63**(1–2), 46–53.

Carroll, D. F. & Tressler, R. E. (1988). Effect of creep damage on the tensile creep behavior of a siliconized silicon carbide. *J. Am. Ceram. Soc.*, (in press).

Carter, C. H., Jr., Davis, R. F. & Bentley, J. (1984). Kinetics and mechanisms of high temperature creep in silicon carbide: I, reaction-bonded. *J. Am. Ceram. Soc.*, **67**(6), 409–17.

Chen, C. F. & Chuang, T.-J. (1987). High temperature mechanical properties of SiA10N ceramic, creep characterization. *Cer. Eng. and Sci. Proc.*, **8**(7–8), 796–804.

Christ, B. W. & Swanson, S. R. (1978). Alignment problems in the tensile test. *J. Test. and Evaluation*, **4**(6), 405–17.

Cohrt, H., Grathwohl, G. & Thummler, F. (1984). Non-stationary stress distribution in a ceramic bending beam during constant load creep. *Res Mechanica*, **10**, 55–71.

Chuang, T.-J., Wiederhorn, S. M. & Chen, C. F. (1987). Transient behavior of structural ceramics under flexural creep. In *Proceedings of the Third International Conference on Creep and Fracture of Engineering Materials and Structures*, ed. B. Wilshire & R. W. Evans, The Institute of Metals, London, pp. 957–73.

Chuang, T.-J. & Wiederhorn, S. M. (1988). Damage-enhanced creep in a siliconized silicon carbide: mechanics of deformation. *J. Am. Ceram. Soc.*, **71**(7), 595–601.

Chuck, L. (1986). Private communication.

Govila, R. K. (1983). Material parameters for life prediction in ceramics. In *Ceramics for High-Performance Applications III, Reliability*, ed. E. M. Lenoe, Plenum Press, New York.

Grathwohl, G. (1984), Regimes of creep and slow crack growth in high temperature rupture of hot pressed silicon nitride. In *Deformation of Ceramic Materials II*, ed. R. E. Tressler & R. C. Bradt, Plenum Press, New York, pp. 573–86.

Hockey, B. J. & Wiederhorn, S. M. (1988). Creep deformation of siliconized silicon carbide. To be published.

Jakus, K. & Wiederhorn, S. M. (1988). Creep deformation of ceramics in four point bending. To be published.

Kossowsky, R., Miller, D. G. & Diaz, E. S. (1975). Tensile and creep strengths of hot pressed Si_3N_4. *J. Mater. Sci.*, **10**, 983–97.

Lange, F. F., Diaz, E. S. & Anderson, C. A. (1979). Tensile creep testing of improved Si_3N_4. *Am. Ceram. Soc. Bull.*, **58**, 845–8.

Lange, F. F., Clarke, D. R. & Davis, B. I. (1980). Compressive creep of Si_3N_4/MgO alloys, Part 2, source of viscoelastic effect. *J. Mater. Sci.*, **15**, 611–15.

Morrell, R. (1972). A tensile creep apparatus for ceramic materials using simple knife-edge universal joints. *J. Physic. Sci. INFT.*, **5**, 465–467.

Morrell, R. & Ashbee, K. H. G. (1973). High temperature creep of lithium zinc silicate glass-ceramics, Part I, general behavior and creep mechanisms. *J. Mater. Sci.*, **8**, 1253–70.

Porter, J. R., Blumenthal, W. & Evans, A. G. (1981). Creep fracture in ceramic polycrystals-I, creep cavitation effects in polycrystalline alumina. *Acta Metall.*, **29**, 1899–1906.

Wakai, F., Sakaguchi, S., Matsuno, Y. & Okunda, H. (1986). Tensile creep test of hot-pressed Si_3N_4. In *Ceramic Components for Engines*, ed. S. Somiya, E. Kanai & K. Adno, Elsevier Applied Science Publishers Ltd, London, pp. 279–85.

Wiederhorn, S. M., Chuck, L., Fuller, E. R., Jr., & Tighe, N. J. (1986). Creep rupture of siliconized silicon carbide. In *Tailoring Multiphase and Composite Ceramics, Materials Science and Research, Vol. 20*, ed. R. E. Tressler, G. L. Messing, C. G. Pantano & R. E. Newnham, Plenum Press, New York, pp. 755–73.

Wiederhorn, S. M., Roberts, D. E., Chuang, T.-J. & Chuck, L. (1988). Damage enhanced creep in a siliconized silicon carbide: phenomenology. *J. Am. Ceram. Soc.*, **71**(7), 602–8.